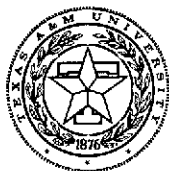


THE APPLICATION OF RIEGELS' RULE AND TIME-LIKE  
DAMPING TO TRANSONIC FLOW CALCULATIONS



aerospace  
engineering  
department

TEXAS A&M UNIVERSITY

by

Donald Lee Herron

Texas A&M University

College Station, Texas



TAMRF-3033-7401

April 1974

(NASA-CR-138181) THE APPLICATION OF  
RIEGELS' RULE AND TIME-LIKE DAMPING TO  
TRANSONIC FLOW CALCULATIONS (Texas A&M  
Univ.) 24 p HC \$4.25 CSDL 20D

N74-21935

Unclas  
G3/12 37903

presented at the 22nd AIAA

Southwestern Student Paper Competition

Arlington, Texas

TEXAS ENGINEERING EXPERIMENT STATION

THE APPLICATION OF RIEGELS' RULE AND TIME-LIKE  
DAMPING TO TRANSONIC FLOW CALCULATIONS

by

Donald Lee Herron

Texas A&M University

College Station, Texas

Spring 1974

### Acknowledgement

This work was partially sponsored by NASA Grant No. NGR-44-001-157. The Technical Officer for the grant is Mr. J. C. South, Jr., Theoretical Aerodynamics Branch, NASA Langley.

11

THE APPLICATION OF RIEGELS' RULE AND TIME-LIKE DAMPING  
TO TRANSONIC FLOW CALCULATIONS

Donald Lee Herron  
Texas A&M University  
College Station, Texas

Abstract

Finite difference relaxation solutions of the nonlinear small perturbation equations have proven reliable and successful in determining the transonic flowfields about thin airfoils. However, application of the small perturbation approach to thick airfoils usually results in an accuracy less than desirable. This paper discusses the incorporation of Riegels' Rule and time-like damping into the small perturbation approach and their application to thick and thin airfoils in transonic flow. Studies for thick and thin airfoils are presented. It is concluded that Riegels' Rule and damping should both be included in small perturbation transonic flow calculations.

## INTRODUCTION

In recent years, considerable research has been performed using transonic small perturbation theory to solve the transonic flow past airfoils. For example, Murman and Cole used this theory to compute the flowfield around thin airfoils including cases with imbedded shocks. <sup>(1)</sup>

They solved the problem of mixed subsonic and supersonic flow regions using a relaxation technique involving a mixed finite difference system. A retarded difference technique was used in supersonic regions to incorporate the mathematical properties of supersonic flow into the difference equation representing the actual differential equation. This new method calculated the velocity at each point in the flowfield and tested it to determine if the flow was subsonic or supersonic at that point. The appropriate hyperbolic or elliptic type difference equation was then selected for that point on the grid. This approach introduced the proper dependence of the differential equation throughout the flowfield and led to a set of simultaneous algebraic equations results that could be solved in an iterative fashion using a line relaxation algorithm. The value of the perturbation potential was found along each vertical line on the grid and the whole process moved in the positive x direction. In this procedure, shock waves appeared naturally. The iteration ended when the process converged to a final answer. Murman and Cole obtained accurate results for thin airfoils using this approach.

Steger and Lomax used a successive line over-relaxation process in the same manner as described by Murman and Cole, because this was more efficient with regard to computing time. <sup>(2)</sup> The complete perturbation velocity potential equation was used along with a transformed coordinate system.

The small perturbation equations have several advantages over the total potential equations. The transformed coordinate system can be a simple one, and the airfoil surface boundary conditions map the axis, thus coinciding with the grid points, which means that mapping is not necessary. Also, the computing time is much shorter, typically by a factor of two, than that required when the full equations are involved. The disadvantage of using the small perturbation equations is that the flowfield calculations tend to become inaccurate and unstable if the flow is not closely aligned with the x axis of the coordinate system because the small perturbation equations are only truly valid for thin, sharp-nosed airfoils. Krupp and Murman demonstrated this fact in the leading edge region of lifting airfoils with high-nose curvature or at moderate to large angles of attack. (3) In other words, these methods do not give good results for thick airfoils.

The purpose of this paper is to deal with these problems by investigating the stability of the small perturbation equations and developing methods of controlling it and by investigating the incorporation of Riegels' Rule into the small perturbation approach so as to permit the study of thick airfoils.

#### FORMULATION OF THE PROBLEM

The equation which describes the small perturbation potential in transonic 2-dimensional flow is

$$\phi_{kx} [(1 - M_\infty^2) - (\gamma + 1) M_\infty^2 \phi_x] + \phi_{yy} = 0 \quad (1)$$

where  $\phi$  is defined such that

$$\begin{aligned} U &= U_\infty (1 + \phi_x) \\ V &= U_\infty \phi_x \end{aligned} \quad (2)$$

Here  $U$  is the velocity component in the  $x$  direction,  $V$  is the velocity component in the  $Y$  direction, and  $U_\infty$  is the free stream velocity.

The transformed coordinate system mentioned earlier puts  $x$  in terms of  $\xi$ , and  $Y$  in terms of  $\eta$ . This transformation is performed in order to save computational time by not having to recalculate the far field boundary conditions periodically throughout the computation. Thus, the infinite domain around the airfoil is transformed into a finite one, i.e.,  $-1 \leq \xi \leq 1$  and  $0 \leq \eta \leq 1$ , by

$$\xi = \tanh \alpha_2 X \quad \eta = \tanh \alpha_1 X$$

Here,  $\alpha_1$  and  $\alpha_2$  are arbitrary constants used to control the stretching.

As a result of the transformation, Eq. (1) becomes

$$\left[ (1 - \xi^2) \phi_{\xi\xi} - 2(1 - \xi^2) \xi \phi_{\xi} \right] \left[ 1 - M_\infty^2 - (\gamma + 1)(1 - \xi^2) \phi_{\xi} \right] \\ + \frac{\alpha_1^2}{\alpha_2^2} (1 - \eta^2)^2 \phi_{\eta\eta} - 2\alpha (1 - \eta^2) \eta \phi_{\eta} = 0 \quad (3)$$

The general boundary conditions are that at the surface of a body the direction of the flow must be tangential to the solid surface, and the velocity potential must return to a value of 0 or  $\frac{-\Gamma}{2\pi}\theta$  at an infinite distance away from the airfoil, depending on whether or not these are non-lifting or lifting conditions. Here,  $\Gamma$  is the circulation.

The finite difference equations are second-order in the elliptic region and first order in the hyperbolic regions and their form depends upon whether or not the flow at a given point is subsonic or supersonic. For subsonic flow, the equations use central difference schemes. A good representation of these can be found in the paper by Murman and Cole (Ref. 1). In supersonic regions, the central difference for  $\phi_{\eta\eta}$  and  $\phi_{\eta}$  are still used but  $\phi_{\xi\xi}$  uses backward differencing in order to currently represent disturbance propagation in supersonic areas.

#### STABILITY ANALYSIS OF THE TRANSONIC SMALL PERTURBATION EQUATION

In examining the iterative solution technique, the change from one iteration to another can be likened to that occurring during some fictitious time step,  $\Delta t$ . Thus, the finite difference equation can be considered as actually representing an equation of the form

$$\nabla\phi_{\xi\xi} + \phi_{\eta\eta} - 2\alpha\phi_{\xi t} - 2\beta\phi_{\eta t} = 0 \quad (4)$$

If the values obtained in a given iteration (denoted as  $\phi^+$ ) are considered to be new and those from the previous iteration (denoted as  $\phi$ ) as old, then  $\alpha$  and  $\beta$  depend upon the combination of new and old values actually used in the difference equations. As time (i.e. number of iterations) becomes large



$\phi_{st}$  and  $\phi_{nt}$  become small and the solution approaches the desired steady state solution.

Now Jameson<sup>(4)</sup> has shown that if

$$S = \xi \quad N = \eta \quad T = t - \frac{\alpha \xi}{V} + \beta \eta$$

$$\frac{\partial}{\partial \xi} = \frac{\partial}{\partial S} - \frac{\alpha}{V} \frac{\partial}{\partial T}, \quad \frac{\partial}{\partial \eta} = \frac{\partial}{\partial N} + \beta \frac{\partial}{\partial T}$$

Then the time dependent equation, Eq. (4), becomes

$$V \phi_{SS} + \phi_{NN} + \left( \frac{\alpha^2}{-V} - \beta^2 \right) \phi_{TT} = 0 \quad (5)$$

In this equation either S or N could be the time-like direction; however, in the actual time invariant equation

$$V \phi_{\xi\xi} + \phi_{\eta\eta} = 0 \quad (6)$$

the coordinate,  $\xi$ , is the desired time-like direction in the supersonic zone. (Note from Eq. (3) that in supersonic zone the coefficient, V, of  $\phi_{\xi\xi}$  is negative). Hence, in Eq. (5) s is the desired time-like coordinate and the coefficients of  $\phi_{NN}$  and  $\phi_{TT}$  must both be positive. This imposes the condition that

$$\alpha^2 > -V\beta^2 \quad (7)$$

in order for the solution to be stable in supersonic regions. Obviously,

if the opposite were true, the equations would become unstable during the iteration process due to  $N$  being the time like coordinate.

Thus, a stability analysis of the present problem, Eq. (3), requires determination of the  $\alpha$  and  $\beta$  terms introduced via the finite difference analogs. This can be accomplished by isolating the new and old  $\phi$ 's in the equation. Hence, the finite difference form of Eq. (3) used in the solution technique can be written as

$$\begin{aligned}
 & DEQ + V_{ij} [(1-\xi^2)^2 \left( \frac{\phi_{ii}^+ - \phi_{ii} - \phi_{i-1,j}^+ + \phi_{i-1,j} - \phi_{i-1,i}^+}{\Delta \xi^2} \right. \\
 & \left. + \frac{\phi_{i-2,i}^+ - \phi_{i-2,i}}{\Delta \xi^2} \right)] + \alpha (1-\eta_j^2)^2 \left( \frac{\phi_{i,j+1}^+ - \phi_{i,j+1} - \phi_{i,j}^+}{\Delta \eta^2} \right. \\
 & \left. + \frac{\phi_{i,j} - \phi_{i,i}^+ + \phi_{i,i} + \phi_{i,j-1} - \phi_{i,j-1}}{\Delta \eta^2} \right) - 2\alpha (1-\eta_j^2) \eta_j \left( \frac{\phi_{i,j+1}^+}{\Delta \eta} \right. \\
 & \left. - \frac{\phi_{i,j+1} - \phi_{i,j-1} + \phi_{i,j-1}}{2\Delta \eta} \right) = 0 \quad (8)
 \end{aligned}$$

where  $i$  and  $j$  represent the  $x$  and  $y$  coordinates of the point in question on the grid. The symbol DEQ represents the finite difference equation and the "+" markings indicate new values calculated in the iteration. Also,

$$V_{ij} = \left[ 1 - M_{\infty}^2 - (\gamma + 1) M_{\infty}^2 \alpha_2^2 (1 - \phi_i^2) \frac{\phi_{i+1,j} - \phi_{i-1,j}}{2 \Delta \xi} \right] \quad (9)$$

is the form of the basic differential equation when it is written entirely in terms of  $\phi$  values from the previous iteration.

By rearranging the terms in Eq. (8), a form results from which  $\alpha$  and  $\beta$  can be recognized. This form is

$$\begin{aligned} \text{DEQ} + \frac{V_{ij} \Delta t}{\Delta \xi} \left[ (1 - \xi^2)^2 \left( \frac{\phi_{\xi t i - \frac{1}{2}} - \phi_{\xi t i + \frac{1}{2}}}{\phi_{\xi t i}} \right) \right] \phi_{\xi t i, j} \\ + \frac{\alpha_1^2}{\alpha_2^2} \frac{(1 - \eta_j^2)^2 \Delta t}{\Delta \eta} \left( \frac{\phi_{\eta t j + \frac{1}{2}} - \phi_{\eta t j - \frac{1}{2}}}{\phi_{\eta t j}} \right) \phi_{\eta t i, j} \\ - 2 \frac{\alpha_1^2}{\alpha_2^2} (1 - \eta_j^2) \eta_j \Delta t \phi_{\eta t} = 0 \quad (10) \end{aligned}$$

Hence,  $\alpha$  is represented by the coefficient of  $\phi_{\xi t}$  while  $\beta$  is represented by the coefficients of  $\phi_{\eta t}$ . The subscript,  $t$ , stands for the time-like nature of the relaxation process and  $\Delta t$  has been introduced to permit the formation of  $\phi_{st}$  and  $\phi_{nt}$ .

Divergence can occur if the requirement of Eq. (7) is violated. If

the slopes are steep, the value of  $(\phi_{nt_j + 1/2} - \phi_{nt_j - 1/2})$  becomes large and  $\beta$  will most likely increase to a point where  $-V\beta^2$  might become larger than  $\alpha^2$ . Also, if a fine grid is used,  $(\phi_{\xi t_i - 1/2} - \phi_{\xi t_i - 3/2})$  tends to approach zero thereby reducing the value of  $\alpha$ . It is seen that both of these cases can and do contribute to the divergence instability problem.

The stability of Eq. (10) can be enhanced by introducing another  $\phi_{\xi t}$  term which essentially increases  $\alpha$  and guarantees the satisfaction of Eq. (7). The term and its differenced form are

$$\epsilon \frac{\Delta t}{\Delta \xi} \phi_{\xi t} = \epsilon \frac{\Delta t}{\Delta \xi} \left( \frac{\phi_{i,j}^+ - \phi_{i,j} - \phi_{i-1,j}^+ + \phi_{i-1,j}}{\Delta t \Delta \xi} \right) \quad (11)$$

where  $\epsilon$  is a damping constant specified to insure a sufficiently large  $\alpha$ . Adding this time-like damping term also helps to make the equation diagonally dominant which also encourages convergence. Addition of the Riegels' Rule will further insure convergence of the problem, and this will be discussed in the next section.

However, it should be noted at this point that the damping used to help convergence is time-like and that the  $\phi_{\xi t}$  and  $\phi_{nt}$  terms go to zero as the number of iterations become large. In this case the damping is not the artificial viscosity type, a term which would appear as  $\phi_{\xi\xi\xi}$  and which would affect the final solution near shock waves.

#### RIEGELS' RULE

It has been shown in the previous section that large slopes on airfoil

surfaces can produce instability when using the small perturbation equations. To obtain good results on thick airfoils, some technique needs to be used to handle the slopes that will maintain stability in the problem and yet not produce inaccuracy in the results. The investigations carried out for this paper incorporated Riegels' Rule into the calculations. Riegels' Rule can be stated as

$$y'_c = \frac{y'_a}{\sqrt{1+c(y'_a)^2}} \quad (12)$$

where  $y'_a$  is the actual slope of the airfoil and  $y'_c$  is the slope used in the computation.  $c$  is a selected constant. Riegels, a German fluid dynamicist, determined that this relationship with  $c = 1$  existed between the actual slopes and the computational slopes when the airfoil was transformed to a slit in the computational plane<sup>(5)</sup>. While small perturbation theory does not transform the airfoil, it does represent it as a slit. Also, as can be seen by Eq. (12), Riegels' Rule has little effect when slopes are small, but it does make a blunt nosed airfoil appear sharp nosed. Thus, it makes the computational airfoil more in line with the restrictions of small perturbation theory.

Mike Hall (NPL, England) through private communication, has reported that using a  $c$  value of 0.2 gave good results in many cases. Thus, this is the value of  $c$  that was used in the cases reported in this paper.

It should be noted that present application of Riegels' Rule is truly empirical and intuitive and that solutions for blunt airfoils may still be in error very near the leading edge. However, the inclusion of Riegels' Rule

might extend the validity of the small perturbation equations used in transonic flow calculations.

## RESULTS

The numerical calculation discussed in this section were designed to investigate the need for inclusion of time-like damping and the applicability and features of Riegels' Rule. Two grid sizes were used in these calculations, a coarse grid with 19 points on each surface of the airfoil and a medium grid with 39 mesh points on each surface.

The first case tested a six percent Biconvex airfoil at  $1^\circ$  angle of attack on a coarse grid at Mach 0.9. Results were obtained with and without Riegels' Rule, and no damping was used in either case. A plot of  $C_p$  at different points along the chord is shown in Fig 1. Notice there are no significant differences in the use or absence of Riegels' Rule. This lack of difference is good because it shows that the incorporation of Riegels' Rule into the solution scheme does not alter the results obtained for thin airfoils, which were good without Riegels' Rule.

It is worthy of note that the pressure distribution shown in Figure 1 indicates the presence of shock waves on both the upper and lower surfaces. Also since the critical  $C_p$  (value at local Mach one) is about  $-0.20$ , much of the flow is supersonic. Finally, it should be recognized that the upper and lower pressures are different and that this is a lifting case.

A nonlifting NACA 0006 airfoil was next investigated in a super critical flow with  $M_\infty$  of 0.85 on the coarse grid system. Fig. 2 shows that there is not much difference in the effect of  $C_p$  when Riegels' Rule is added to the calculations. This trend is probably due to the use of the coarse grid,

and if a finer grid were used it is believed a greater difference could be noticed. Basically, the problem is that when slopes are small  $y'_c$  is not much different than  $y'_a$ . The course grid system does not place any points near the leading edge where the slopes are large, and thus the lack of effect due to Riegels' Rule was anticipated. Nevertheless, the results on Figure 2 appear reasonable.

When a NACA 0012 airfoil is subjected to transonic flow conditions at a freestream Mach number of 0.8 one observes a distinct effect in the calculated results of the incorporation of Riegels' Rule into the small perturbation equations. The resultant  $C_p$  distributions are plotted on Fig. 3. Notice that values of  $C_p$  obtained with and without Riegels' Rule are different near  $x = -.15$ . Since the grid used was coarse, these differences are small; but they do indicate that Riegels' Rule can affect the results obtained with thick round-nosed airfoils.

Up to this point, time-like damping was not included in any of the calculations. The need for this damping arose when it was attempted to use the medium grid size. Calculations using the medium grid produced a divergent solution in a NACA 0006 airfoil at a freestream Mach number of 0.9. This divergence occurred even when Riegels' Rule was used in the equations. Consequently, damping was added to the equations and this resulted in convergence of the solution. A graphic demonstration of the divergence problem and eventual convergence of  $C_p$  is portrayed in Fig. 4. The damping constant,  $\epsilon$ , used in this case was 2.5. Notice the wide differences not only in the magnitudes of the  $C_p$  values but also in the shock location. Also the change in  $\phi$  from one iteration to the next in the

divergent case was never less than  $10^{-2}$ , while in the damped case the change in  $\phi$  at the end of the calculation was less than  $10^{-5}$ . Also, without adding the damping term,  $\phi_{st}$ , the incorporation of Riegels' Rule would have been fruitless.

The importance of using both Riegels' Rule and time-like damping is seen in Fig. 5. Here the flow about a NACA 0012 airfoil was computed at an angle of attack of  $0^\circ$  at a Mach number of 0.8 on a medium grid. On this particular plot, the solution to the full potential flow equations, obtained by Dr. L. A. Carlson of Texas A&M University, is also included and can be compared to the results obtained using the small perturbation equations. It should be noted that without the addition of time-like damping to the process, solutions for this case did not converge. This point is significant because it shows the need for damping in calculations for thick airfoils with small grid spacing. Figure 5 also shows the importance of including Riegels' Rule when using small perturbation equations. Using the equations without Riegels' Rule yields values of  $C_p$  considerably different than those obtained using the full equations. However, by incorporating Riegels' Rule into the small perturbation equations, a close approximation of the full potential equation solution is obtained.

It should be noted that the solutions shown on Fig. 5 may not be totally accurate due to the sensitivity of thick airfoil results to grid size and grid spacing. Nevertheless, the agreement between the small perturbation solution with Riegels' Rule and the solution from the full equation serves to justify the usage of Riegels' Rule since both sets of results were obtained using the same grid size and spacing. Thus, any inaccuracies due to grid choice are present in both sets of calculations.



It is hoped in the near future to further verify these results by studying thick airfoils at angles of attacking using a fine grid. A typical example would be an NACA 0012 at  $\alpha = 2^\circ$  and  $M_\infty$  of 0.75.

#### CONCLUSIONS

Based upon these initial studies the following conclusions can be stated:

- (1) The inclusion of Riegels' Rule does not change or decrease the accuracy obtained for small perturbation solutions for thin airfoils.
- (2) The addition of time-like damping to equations enhances the stability of the iterative process.
- (3) In small perturbation calculations for the flow about thick blunt-nosed airfoils, time-like damping is frequently required in order to maintain stability and achieve a convergent solution.
- (4) The inclusion of Riegels' Rule in the small perturbation solution leads to results for blunt airfoils that are in agreement with those obtained for the complete equations.

Thus, it is recommended that when using small perturbation methods for transonic flow calculations about blunt, thick airfoils that Riegels' Rule and time-like damping both be included.

REFERENCES

1. Murman, E. M. and Cole, J. D., "Calculation of Plane Steady Transonic Flows", AIAA Journal, Vol. 9, No. 1, Jan. 1971, pp. 114-121.
2. Steger, J. L. and Lomax, H., "Transonic Flow about Two-Dimensional Airfoils by Relaxation Procedures", AIAA Journal, Vol. 10, No. 1, Jan. 1972, pp. 49-54.
3. Krupp, J. A. and Murman, E. M., "Computation of Transonic Flows Past Lifting Airfoils and Slender Bodies", AIAA Journal, Vol. 10, No. 7, July 1972, pp. 880-886.
4. Jameson, A., "Numerical Calculation of the Three Dimensional Transonic Flow Over a Yawed Wing," Proc. AIAA Computational Fluid Dynamics Conference, July 19-20, 1973.
5. Riegels, F., "Das Umströmungsproblem bei inkompressiblen Potentialströmungen," Ingenieur-Archiv, Vol. 16, 1948, p. 373.

ACKNOWLEDGMENTS

I wish to extend my sincere gratitude to Dr. Leland A. Carlson of the Aerospace Engineering Department at Texas A&M University who provided much assistance and inspiration in the preparation of this paper.

Also, I wish to thank Raymond Luh, an undergraduate student at Texas A&M, for his assistance in the preparation of the figures.

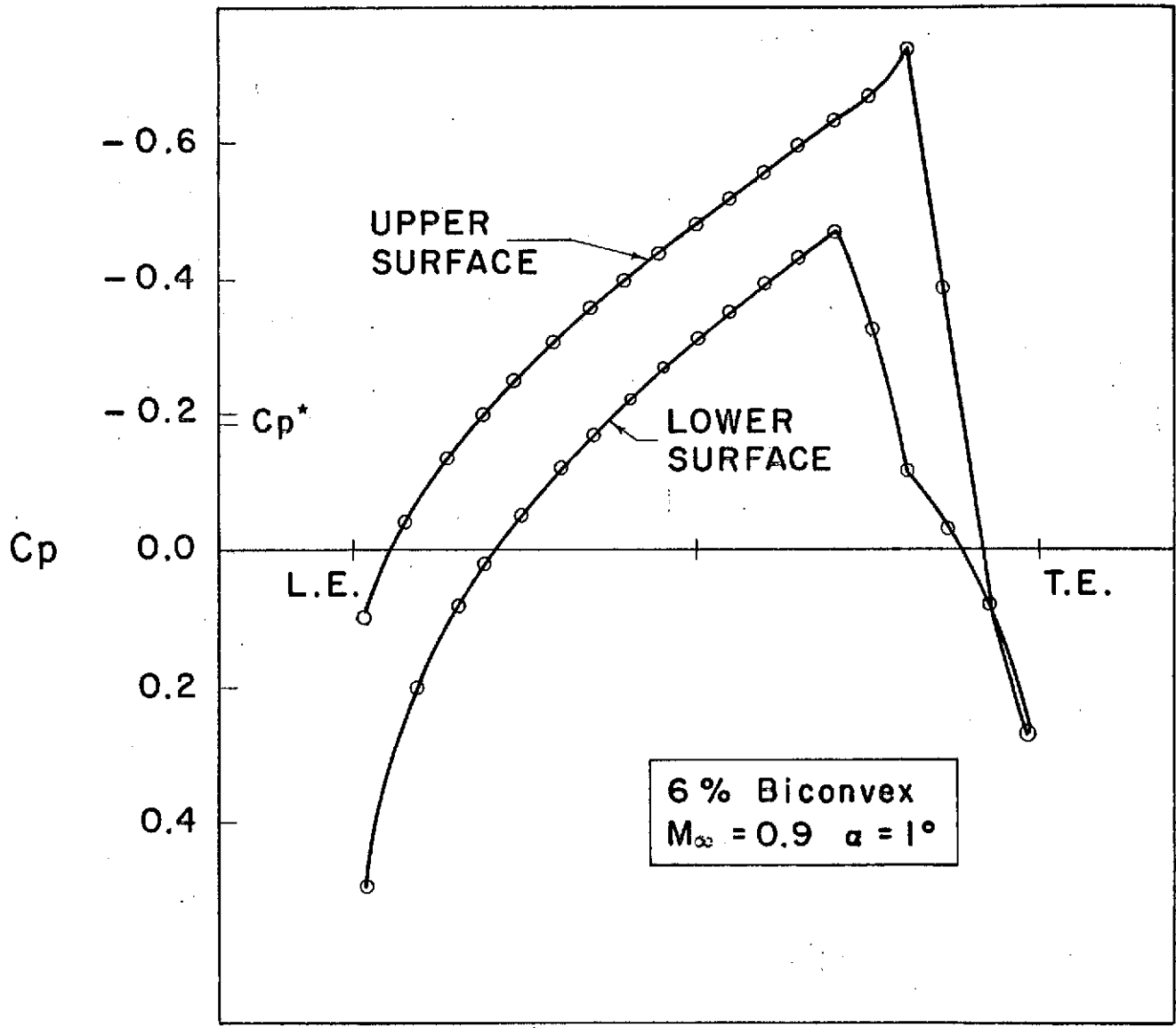


FIGURE 1  
THE VARIATION OF  $C_p$  ALONG THE CHORD OF A  
6% BICONVEX (WITH AND WITHOUT RIEGEL'S RULE)

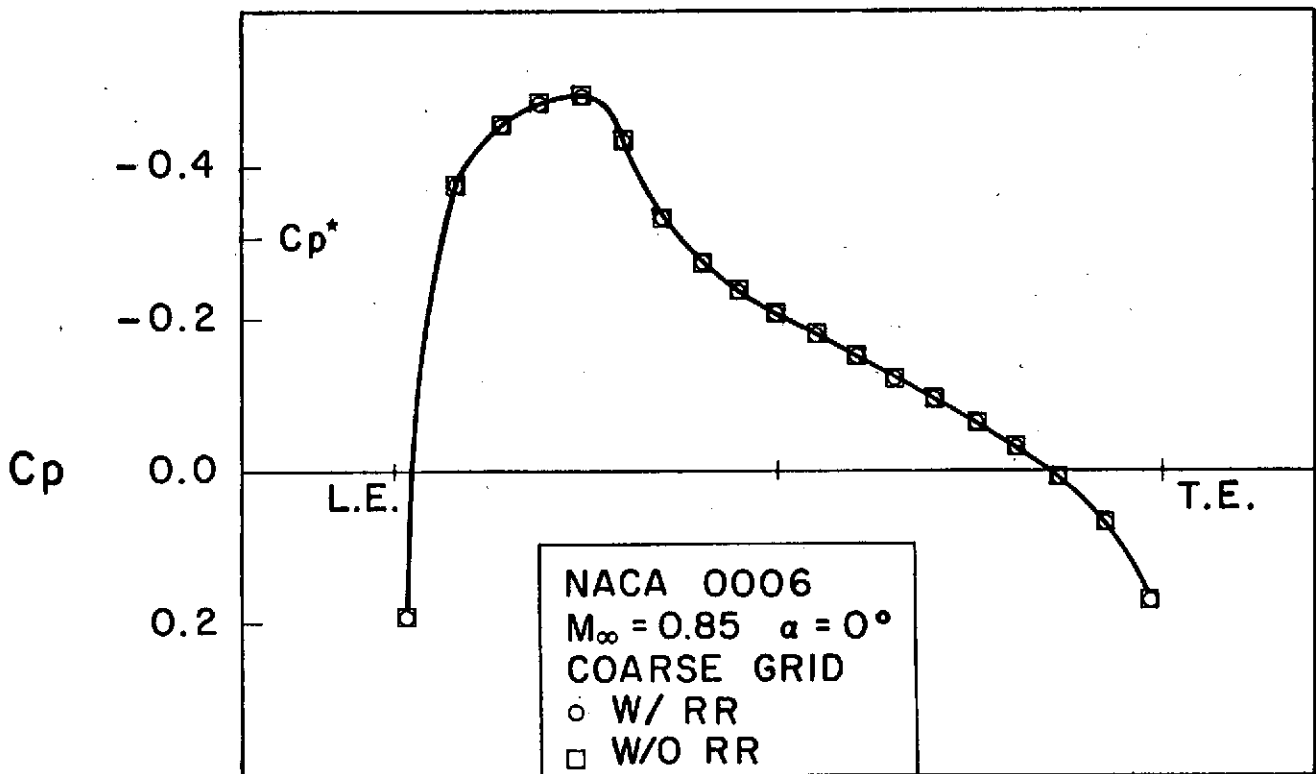


FIGURE 2

THE VARIATION OF  $C_p$  ALONG THE CHORD OF A  
 NACA 0006 (WITH AND WITHOUT RIEGEL'S RULE)

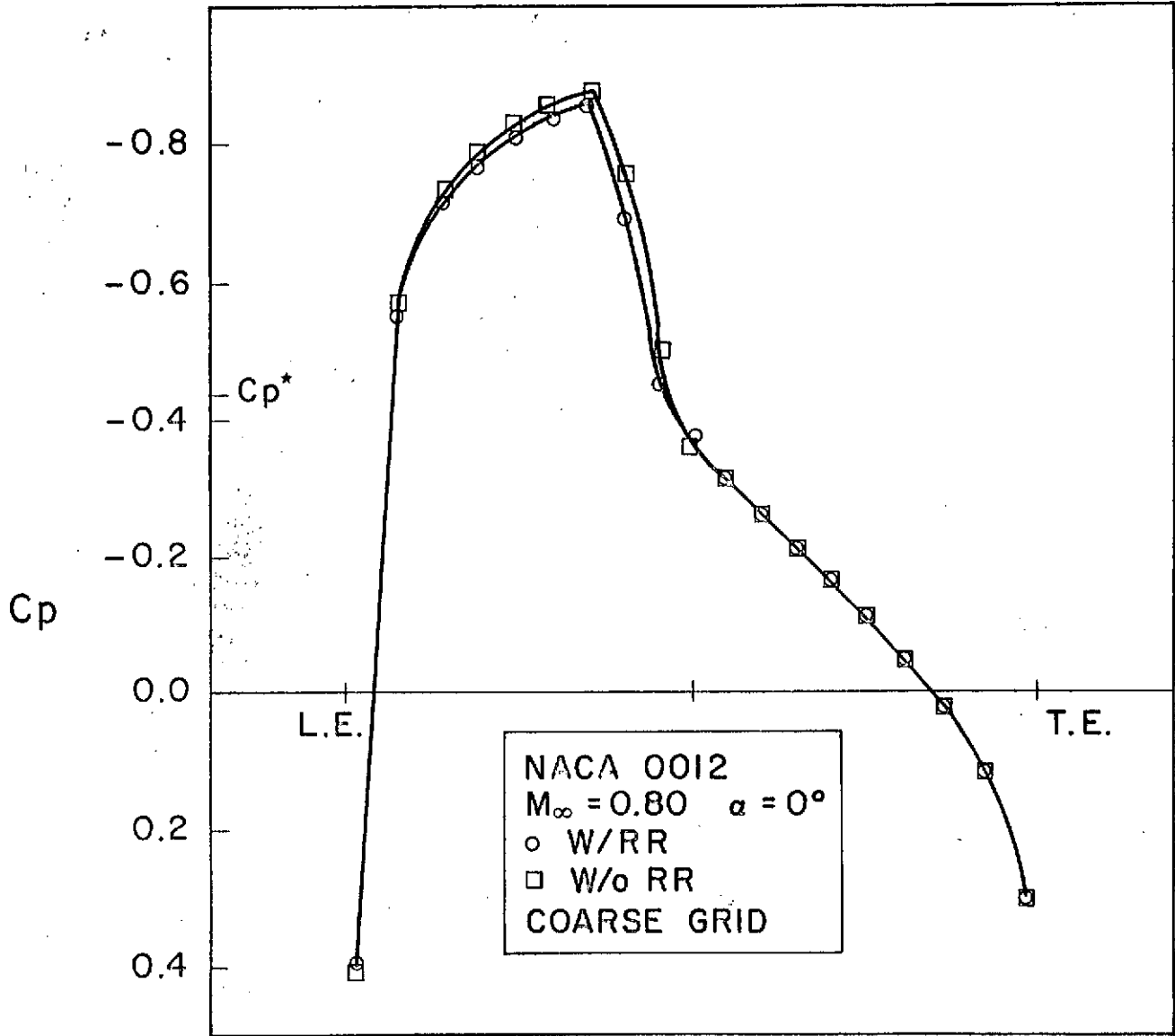


FIGURE 3

THE VARIATION OF  $C_p$  ALONG THE CHORD OF A  
NACA 0012 (WITH AND WITHOUT RIEGEL'S RULE)

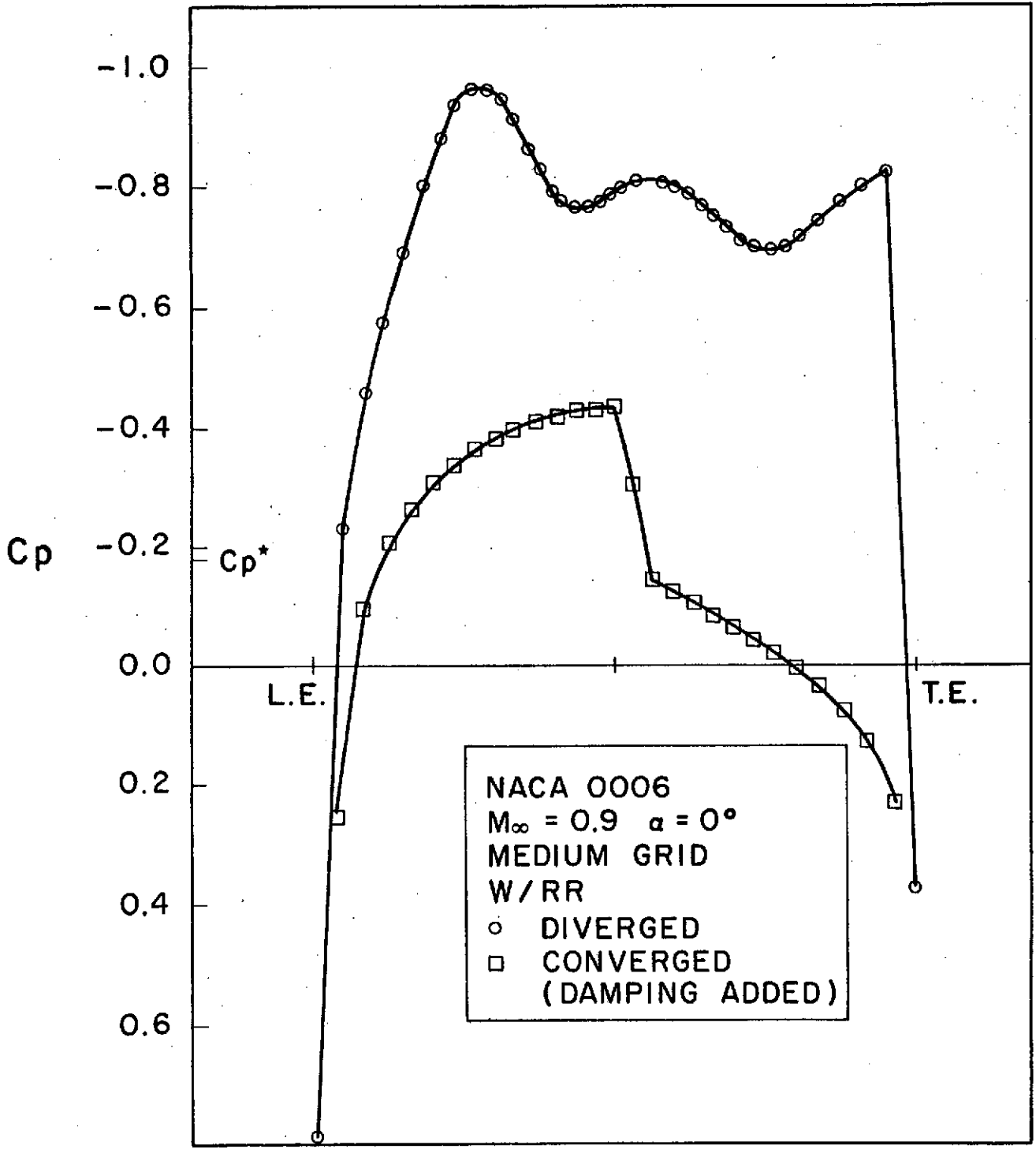


FIGURE 4

THE EFFECT OF TIME-LIKE DAMPING IN THE SMALL  
PERTURBATION EQUATIONS ON NACA 0012 RESULTS  
(WITH RIEGEL'S RULE)

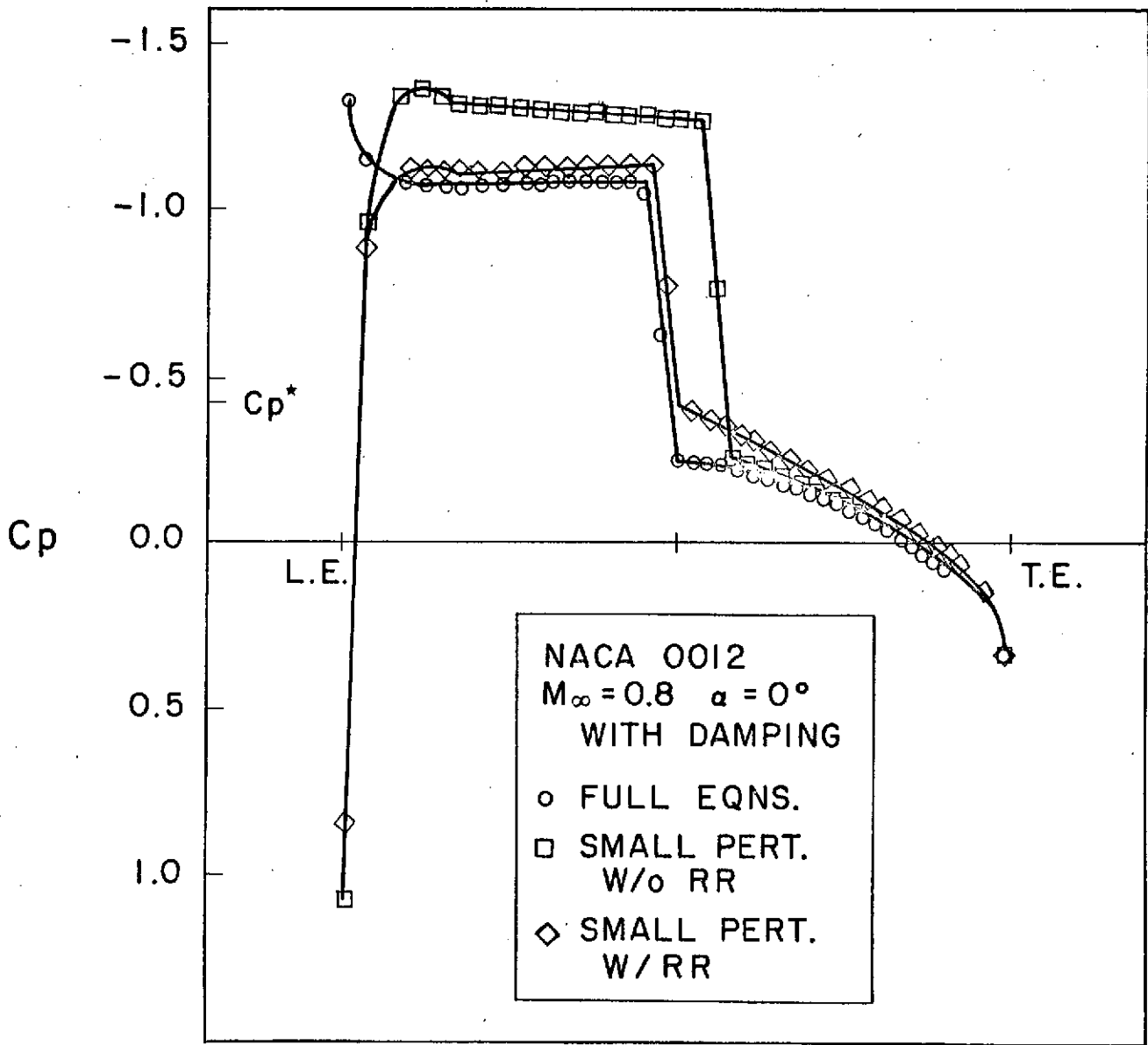


FIGURE 5  
THE EFFECT OF RIEGEL'S RULE IN THE SMALL  
PERTURBATION EQUATIONS ON NACA 0012 RESULTS  
(WITH DAMPING)